Dynamic Mechanical Responses of *Arabidopsis* Thylakoid Membranes during PSII-Specific Illumination

Casper H. Clausen,[†] Matthew D. Brooks,[‡‖] Tai-De Li,[†] Patricia Grob,[‖] Gigi Kemalyan,[‖] Eva Nogales,[§¶‖] Krishna K. Niyogi,[‡§‖] and Daniel A. Fletcher[†§*]

[†]Bioengineering Department and [‡]Department of Plant and Microbial Biology, University of California, Berkeley, California; [§]Physical Biosciences Division, Lawrence Berkeley National Laboratory, Berkeley, California; [¶]Molecular and Cell Biology Department, University of California, Berkeley, California; and [‖]Howard Hughes Medical Institute, University of California, Berkeley, California

ABSTRACT Remodeling of thylakoid membranes in response to illumination is an important process for the regulation of photosynthesis. We investigated the thylakoid network from *Arabidopsis thaliana* using atomic force microscopy to capture dynamic changes in height, elasticity, and viscosity of isolated thylakoid membranes caused by changes in illumination. We also correlated the mechanical response of the thylakoid network with membrane ultrastructure using electron microscopy. We find that the elasticity of the thylakoid membranes increases immediately upon PSII-specific illumination, followed by a delayed height change. Direct visualization by electron microscopy confirms that there is a significant change in the packing repeat distance of the membrane stacks in response to illumination. Although experiments with Gramicidin show that the change in elasticity depends primarily on the transmembrane pH gradient, the height change requires both the pH gradient and STN7-kinase-dependent phosphorylation of LHCII. Our studies indicate that lumen expansion in response to illumination is not simply a result of the influx of water, and we propose a dynamic model in which protein interactions within the lumen drive these changes.

INTRODUCTION

The mechanisms controlling how a plant acclimates to light and maintains photosynthetic efficiency are of great interest for understanding photosynthesis. The photosynthetic machinery used to convert light to chemical energy is located in the chloroplast, with reactions carried out by pigment-protein complexes in the thylakoid membrane network. Imbalances between the amount of light that is absorbed by the photosystems and the amount that can be used for photosynthesis necessitate multiple mechanisms to dissipate excess energy (1).

Photosynthetic organisms respond to changes in light intensity and wavelength by several processes, including energy-dependent quenching of chlorophyll (1–3) and state transitions of thylakoid membranes (4). Although certain aspects of these processes have been extensively studied, many others are not yet fully understood (5). A particular area of recent interest is how the light-harvesting complex of photosystem II (LHCII) and the thylakoid membrane are reorganized in response to light to protect the plant from damage, optimize electron transport, and facilitate repair (6–8). One of the proposed mechanisms behind these changes of the thylakoid membrane involves phosphorylation and movement of LHCII, which is thought to balance light harvesting of Photosystem I (PSI) and Photosystem II (PSII) by both molecular and ultrastructural reorganization (6,7,9).

The effects on thylakoid membrane remodeling as a result of illumination with PSI- and PSII-specific wavelengths have been intensely investigated (6,7,10,11). Research has focused on identifying structural changes occurring in thylakoid membranes before and after illumination using techniques such as fluorescence microscopy, electron microscopy (EM), or atomic force microscopy (AFM) (6,7,12). AFM has been used in previous studies to image the composition of the thylakoid membrane (10,13), the thylakoid superstructure (6,14,15), and changes in the protein arrangement (16). However, there are no reports describing isolated thylakoid mechanical properties or the dynamics of structural remodeling occurring in response to light in real time.

In this study, we have characterized the changes in thylakoid membrane mechanical properties occurring during a state transition in response to PSII-specific illumination. The height and elasticity changes of isolated thylakoid networks were investigated in liquid using an AFM customized for rheology measurements, in which the cantilever was held in contact with the sample at a constant force to measure height changes and a small sinusoidal movement of the cantilever was applied to capture viscoelastic properties of the thylakoid membrane. An inverted optical microscope was used to control illumination wavelength and intensity and to obtain chlorophyll fluorescence images of the thylakoid membrane, and EM provided a description of the membrane ultrastructure before and after illumination.

MATERIALS AND METHODS

Plant material

Arabidopsis thaliana wild-type (WT) (Col-0) and *stn7* plants (17) were grown in 7.5-cm soil pots in a chamber with a 10-h day, 14-h night cycle

Submitted September 3, 2013, and accepted for publication March 10, 2014.

*Correspondence: fletch@berkeley.edu

Editor: Jochen Guck.

0006-3495/14/05/1864/7 $2.00

http://dx.doi.org/10.1016/j.bpj.2014.03.016

at 21.5°C and a light intensity of 150 μmol photon m^{-2} s^{-1}. Plants were used for experiments before bolting at an age of 7–10 weeks.

Thylakoid isolation

Thylakoid membranes were isolated according to Casazza et al. (18). The whole preparation was carried out at 4°C and in the dark. Leaves from *Arabidopsis* plants (10–20 g) as well as all the equipment used were cooled to 4°C 1 h before the isolation process. The leaves were shredded in a blender by eight 0.5-s pulses in 100 ml buffer, containing 0.4 M sorbitol, 5 mM EGTA, 5 mM EDTA, 5 mM $MgCl_2$, 10 mM $NaHCO_3$, and 20 mM Tricine at pH 8.4. The mixture was filtered through six layers of cheesecloth, and at the end the cloth was gently squeezed to obtain a higher yield. The solution was centrifuged for 3 min at 2600 × *g*. The supernatant was discarded, and the pellet was resuspended in 10 mL of resuspension buffer containing 0.3 M sorbitol, 2.5 mM EDTA, 5 mM $MgCl_2$, 10 mM $NaHCO_3$, 20 mM HEPES at pH 7.6. This step was repeated three times. After the last centrifugation, the supernatant was discarded, and the pellet was resuspended for 5 min in 10 mL of hypotonic buffer containing 2.5 mM EDTA, 5 mM $MgCl_2$, 10 mM $NaHCO_3$, 20 mM HEPES at pH 7.6. The solution was then centrifuged for 3 min at 200 × *g*, and the supernatant was collected and centrifuged for 3 min at 2600 × *g*. Finally, the supernatant was discarded, and the pellet was resuspended in measuring buffer containing 0.3 M sorbitol, 5 mM $MgCl_2$, 10 mM $NaHCO_3$, 20 mM HEPES at pH 7.6. To keep the thylakoid membranes active, the experiments were carried out within 2 h of isolation.

AFM measurements and fluorescence imaging

Before the experiments, glass coverslips were coated with poly-L-lysine by adding 0.1% (w/v) poly-L-lysine solution on the coverslips for 30 min and then washed with measuring buffer four times. The suspension containing the thylakoid membranes was added and left to settle for 10 min followed by four washing steps with the buffer used during the AFM measurements. An incubation period of 10 min was used for the supplementation of electron acceptors (10 μM ferredoxin and 0.6 mM $NADP^+$) and uncoupler (gramicidin D) to the buffer used during the AFM measurements. Polystyrene beads (5 μm diameter) were attached (glued, Norland 61) to a tipless uncoated cantilever (Veeco, customized MLCT cantilever with a nominal spring constant of 0.01 N/m), and their spring constants were individually determined by the thermal vibration method before each measurement (19). The experiments were carried out at room temperature in the dark. Samples were mounted on a Zeiss Observer Z1 microscope. The excitation wavelengths were 484 nm (S484/15×, Chroma), 640 nm (ET640/30×, Chroma), and 740 nm (HQ740/40×, Chroma) for chlorophyll fluorescence imaging, PSII excitation, and PSI excitation. The fluorescence was passed through a long-pass filter (HQ665LP, Chroma). The intensity of the illumination, which was 150 μmol photons m^{-2} s^{-1} for the 640 nm light and 100 μmol photons m^{-2} s^{-1} for the 740 nm light, was measured with a power meter (Melles Griot 13PEM001). Optical images were acquired with an EM CCD camera (Andor Ixon+).

Height and rheology measurements were simultaneously monitored with an AFM (Bruker Bioscope Catalyst) customized for measuring mechanical properties. The wavelength of the AFM laser is 850 nm, which is not absorbed by thylakoid membranes (20). The AFM was mounted on the inverted microscope so that the sample could be imaged by epifluorescence without obstruction by the cantilever (Fig. 1 *A*). To monitor the height change of the thylakoid membranes, the polystyrene bead was in contact with the thylakoid membrane at a constant average force of 0.2 nN (corresponding to ~0.14 μm indentation or ~6% strain) that was maintained by feedback control. To measure viscoelastic properties, we used a rheological technique in which a sinusoidal oscillation with amplitude of 20 nm was applied to the cantilever vertically at 2 Hz. The amplitude and phase shift of the oscillatory cantilever deflection caused by viscoelasticity of the thylakoids was detected

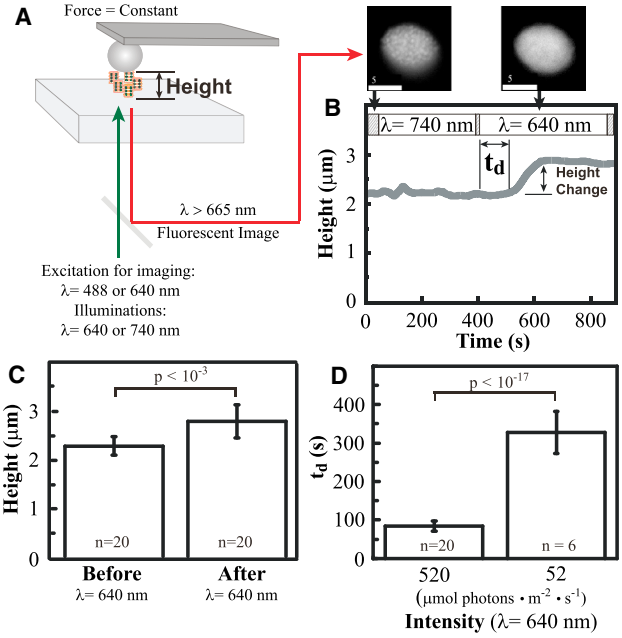

FIGURE 1 Height change of isolated thylakoid membranes in response to PSII-specific illumination. (*A*) Diagram of the experiment showing isolated thylakoid membranes illuminated and imaged by an inverted microscopy, whereas the height (h) is measured by AFM. The fluorescence image shows reduced punctate structures after PSII-specific illumination (640 nm), indicating that unstacking has occurred. Scale bar = 5 μm. (*B*) A typical height response from a thylakoid membrane sample exposed to PSII-specific illumination. There is a time delay (t_d) between the light and the height change of the thylakoid membrane. (*C*) Average height of 20 thylakoid membranes before and after the PSII-specific illumination. (*D*) Average of the time delay at different light intensities. (1 μmol photons = 186.6 mJ for 640 nm light) To see this figure in color, go online.

with a lock-in amplifier (Signal Recovery 7270) and recorded every 10 ms. Nearly constant force was maintained during the periodic oscillations by setting a low gain in the force feedback control software. The time constant of the lock-in amplifier was 1 s with the sensitivity at 500 mV. The AFM measurements were controlled and recorded with a LabView program together with a National Instrument DAQcard (PCI-6229) and an electronic signal filter (Krohn-Hite 3364). For the analysis of the storage and loss moduli, calculations were based on the extended common Hertz model (21). The elastic and viscous moduli were determined by,

$$G^* = \frac{(1-\nu)\cdot k\cdot A}{4\cdot\delta\cdot\sqrt{R\delta_0}}\cdot\exp(i\cdot\phi), \qquad (1)$$

where G^* is the dynamic modulus, ν is the Poisson's ratio assumed to be 0.5 (21), k is the spring constant of the cantilever, A is the measured amplitude, R is the radius of the bead, δ_0 is the average indentation, δ is given as applied amplitude minus the measured amplitude, and ϕ is the phase of the measured signal. The elastic and viscous moduli are the real (G') and imaginary (G'') components of G^*, respectively. Details of the derivation are provided in the Supporting Material.

Electron microscopy

Thylakoid membranes were prepared as described previously and kept in the dark before the experiments. They were illuminated for 5 min with 640 nm light at 150 μmol photons m^{-2} s^{-1} using a Schott KL 1500 LCD

mounted with a 640 nm filter (ET640/30×, Chroma). After illumination the thylakoid membranes were spun down at 2600 *g* for 3 min at 4°C. The supernatant was removed and a small volume of resuspension buffer containing 10% bovine serum albumin cryoprotectant was added to resuspend the pellet. The thylakoid membranes were then pipetted into aluminum Type A specimen carriers (3 mm diameter, 0.5 mm thickness, 0.1 mm cavity, #241, Technotrade International,), covered with Type B aluminum specimen carriers (3 mm diameter, 0.5 mm thickness, 0.3 mm a cavity, #479, Technotrade International) and high-pressure frozen with a Baltec HPM010 before chemical fixation and resin embedding. The frozen samples were transferred to cryovials containing a liquid N_2-frozen fixative cocktail consisting of 1.0% osmium tetroxide and 0.1% uranyl acetate in 100% acetone, and quick-freeze substituted for 90 min (22). After reaching room temperature, the samples were rinsed 3 times in 100% acetone for 5 min, and then infiltrated with Eponate 12 resin, embedded in molds, and polymerized at 60°C for 48 h. The resin blocks were thin sectioned at 60 nm with a Leica UC7 ultramicrotome, and sections were placed onto 3 mm Formvar and carbon-coated copper grids. Grids were poststained with 2% uranyl acetate and 0.1% Reynold's lead citrate. The thylakoid thin sections were imaged with an FEI Tecnai 12 transmission electron micrscope operated at an accelerating voltage of 120 kV and images were collected using 18,500× magnification on a TemCam-F416 (TVIPS), resulting in a 0.58 nm pixel size at the specimen level.

After visual inspection, the transmission electron microscopy images showing thylakoid membranes with the best contrast were selected. Thylakoid stacks were picked manually using the boxer feature within the EMAN software package (23) and individually boxed out for further analysis using the Spider software package (24). The resolution in the EM images of the resin-embedded sections allowed us to quite accurately measure the repeat representing the average sum of the lumenal and stromal spacings for each stack, which was characteristic for each type of sample, but it was not systematically possible to resolve individual thylakoid membranes or individual protein complexes in the lumen (illustrated in Fig. S1 *A*). Briefly, a Radon transform (Spider RM 2DN) of each individual stack was calculated. Each line of coordinate Y in the Radon transform image corresponds to the one-dimensional (1D) projection of the input two-dimensional image along the projection direction Y (angle in degrees). The projection angle increment used was one degree. The strongest line for a straight pattern such as parallel line stacks is obtained for the projection direction parallel to the lines. Additionally, the corresponding Y position gives the orientation of the stack. The strongest line was found in each Radon transform by a simple peak search and extracted, and its average spacing distance was determined by finding the peaks in its 1D Fourier transform amplitudes (Fig. S1 *B*). The use of the Radon transform simplified the stacking distance measurement by reducing it to a simple 1D search in the final Fourier amplitudes. This allowed us to quickly and reliably process a large number of images for each sample. Repeat distances were measured for a total of 103, 155, 105, and 140 stacks for WT samples in light and in the dark, and for *stn7* mutant samples in light and in the dark, respectively. Histograms of the distance distributions were calculated in MATLAB (The MathWorks, Natick, MA) using 1 nm binning. The average repeat distances and errors were obtained from the means and standard deviations of single (WT dark, *stn7* dark and light) or double (WT light) normal distributions fitted to the data (gmdistribution.fit). A one-sided Student *t*-test was performed to ascertain the significance of the repeat distance increase between data sets corresponding to dark versus light-exposed specimens.

RESULTS

Thylakoid membrane height increases in response to PSII-specific light

Isolated thylakoid membranes were illuminated and imaged on an epifluorescence microscope coupled to an AFM for simultaneous height and mechanical property measurements (Fig. 1 *A*). Upon illumination at a wavelength that excites PSII ($\lambda = 640$ nm), dark-adapted thylakoid membranes isolated from individual chloroplasts exhibited a distinct change in height. The membrane structural change was also visible in fluorescence images (*inset*, Fig. 1 *A*). The height change occurred after a time delay (t_d), and reached a stationary height (Fig. 1 *B*). No further change in the height was seen when measurements continued for 30 min after the light was turned off (see Fig. S2). The height of the sample increased by 0.51 ± 0.28 μm (mean ± SD), which represents a 20% increase in height (Fig. 1 *C*), after an average time delay of 84 ± 14 s. Illumination of dark-adapted thylakoid membranes with a wavelength that excites PSI ($\lambda = 740$ nm) did not cause a height increase (Fig. 1 *B*). The t_d depends on the intensity of the PSII-specific light (Fig. 1 *D*), although the magnitude of the height increase is not dependent on the intensity.

Thylakoid membrane elasticity increases in response to PSII-specific light

The elasticity of isolated thylakoid membranes was measured by AFM microrheology (Fig. 2 *A*) at the same time as height was measured. A typical measurement of a WT thylakoid membrane showed that the elasticity started to increase immediately upon illumination with PSII light and reached a maximum after a response time t_r (Fig. 2 *B*). Average thylakoid membrane elasticity increased from

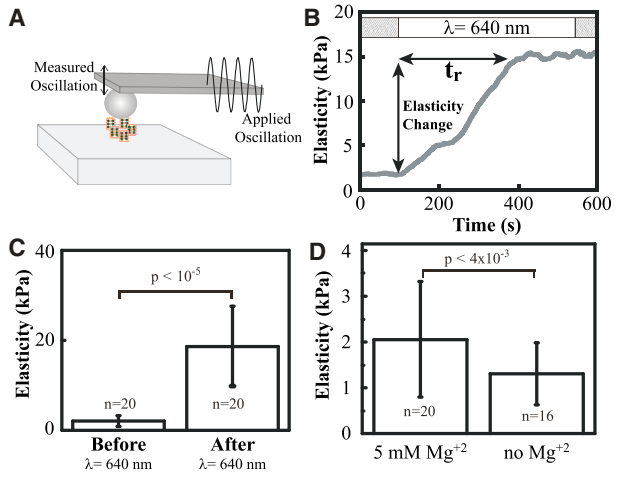

FIGURE 2 Elasticity change of thylakoid membranes in response to PSII-specific illumination. (*A*) Diagram of the experiment showing the microrheology measurement, in which the response of a sample to an oscillatory deformation can be used to calculate elastic properties. (*B*) Typical mechanical response from a thylakoid membrane exposed to PSII-specific illumination. The average response time of the elasticity change (t_r) was 311 ± 36 s (mean ± SD). The elastic and viscous moduli are the real ($\overline{G}'$) and imaginary ($\overline{G}''$) components of $\overline{G}^*$ respectively. (*C*) Average elasticity of 20 thylakoid membranes before and after exposure to light. (*D*) Average elasticity of dark-acclimated thylakoid membranes in the presence and absence of Mg^{2+}. To see this figure in color, go online.

2 ± 1.3 kPa to 18.7 ± 8.9 kPa (mean ± SD) (Fig. 2 *C*). The t_r and rate of elasticity increase were both dependent on illumination intensity (see Fig. S3). No change in the elasticity was observed after the PSII light was turned off for 30 min. Unlike the height response, there was no time delay for the elasticity increase, but it took longer to reach the elasticity maximum than the height maximum. Viscosity changes in the thylakoid were also measured at the same time as elasticity (see Fig. S4).

Thylakoid stacking is known to depend strongly on cation concentrations, and unstacking of thylakoid membranes due to Mg^{2+} depletion has been reported (25). When WT thylakoid membranes were exposed to 640 nm illumination in the absence of Mg^{2+}, there was a modest decrease in elasticity compared to samples in the presence of Mg^{2+} (Fig. 2 *D*). Furthermore, the Mg^{2+}-depleted thylakoids had a lower height compared to nondepleted membranes in agreement with previous reports (6) (Fig. 2 *D*).

Height and elasticity changes are modulated by the pH gradient and STN7-dependent phosphorylation

To investigate the mechanisms responsible for the height and elasticity changes, we carried out experiments on thylakoid membranes isolated from the *stn7* mutant. This mutant lacks the kinase responsible for phosphorylating LHCII in response to unbalanced excitation of PSII relative to PSI, and thus the mutant is defective in state transitions (17). Transmission EM images of WT and *stn7* thylakoids that were either dark-adapted or exposed to PSII-specific illumination confirmed that the changes in membrane stacking previously reported for whole leaves (10) and isolated thylakoids (6) were reproducible in our experiments (Fig. 3, *A* and *B*). Microrheology measurements of the *stn7* mutant showed a larger elasticity change than the WT thylakoid membranes.

To test the role of the pH gradient in the observed elastic response, we treated thylakoids from WT plants with gramicidin D to allow monovalent cations, including protons, to flow across the membrane and prevent the formation of the pH gradient. In contrast to the results with the *stn7* mutant, treatment with gramicidin D prevented an elasticity change upon PSII-specific illumination (Fig. 3 *C*). Interestingly, the height change of both the *stn7* mutant and the gramicidin-treated WT samples was only 5 ± 4% (mean ± SD) after PSII-specific illumination, compared with 22 ± 12% (mean ± SD) in untreated WT thylakoids (Fig. 3 *D*).

This is consistent with EM images showing more profound changes in organization for WT membranes, with a significant increase in both the average and the variability of the stacking distance after light treatment, compared to what is seen for the *stn7* mutant (Fig. 3, *A* and *B*). In WT thylakoids, the stacking spacing repeat increased from 20 ± 10 nm (*dark*) to 21.3 ± 10 nm up to 27 ± 10 nm after light exposure, whereas in the *stn7* mutant the spacing

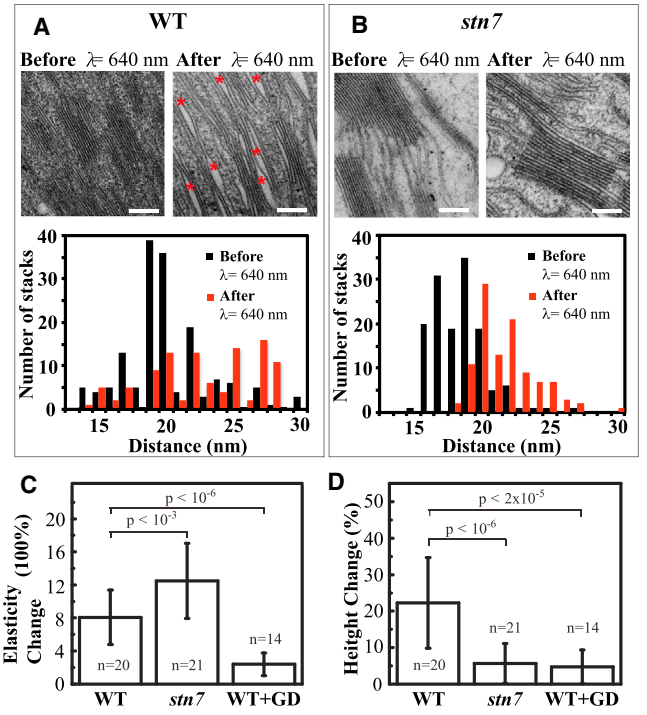

FIGURE 3 Disruptions in membrane stacking affect elasticity and height changes. (*A*) Transmission EM images and histogram plot of changes in the thylakoid ultrastructure of the WT. Bar = 200 nm. (*B*) Transmission EM images and histogram plot of changes in the thylakoid ultrastructure of the *stn7* mutant. Bar = 200 nm. Unstacked regions in the thylakoid images are marked by red stars. Histogram plots of the number of stacks measured versus the membrane-to-membrane distance for dark and illuminated WT and *stn7* thylakoids from EM images. (*C*) Percentage changes in elasticity ($\Delta G'$) of WT, *stn7*, and WT treated with gramicidin D (GD). The average G' of dark adapted samples was 2.06 ± 1.26 kPa for WT, 2.06 ± 0.99 kPa for *stn7*, and 2.72 ± 1.44 kPa for WT treated with gramicidin D. (*D*) Percentage changes in height (Δh) of WT, *stn7*, and WT treated with gramicidin D. The average height of dark adapted samples were 2.28 ± 0.19 μm for WT, 2.27 ± 0.13 μm for *stn7*, and 2.61 ± 0.70 μm for WT treated with gramicidin D. To see this figure in color, go online.

increased only from 18 ± 4 nm (*dark*) to 22 ± 5 nm (*light*) (mean ± SD), both significant increases with better than 99% confidence according to a Student's *t*-test. Additionally, significantly more unstacking was observed after light exposure in the WT thylakoids than in any other condition, as illustrated in Fig. 3 *A*, right panel (*wider white spaces marked by red stars*). The wider spacing observed only in this condition is probably also attributable to a partial thylakoid membrane unstacking. Despite the difference in height change compared to the WT, the *stn7* mutants and gramicidin-treated thylakoid membranes showed no significant difference in the amount of time it took to reach maximum elasticity compared to WT samples (Fig. S5).

DISCUSSION

Our study of the thylakoid membrane physical properties show that exposure to PSII-specific illumination causes an

immediate increase in membrane elasticity and a delayed increase in membrane height. As summarized schematically in Fig. 4, membrane elasticity increased 10-fold relative to the original elasticity over ~311 ± 36 s, whereas the membrane height increased 22 ± 12% over ~84 ± 14 s (mean ± SD) (*data* from Figs. 1 and 2). The rate of the elasticity change and the delay in the start of height changes were found to be dependent on intensity of the PSII-specific illumination. The height increase of the thylakoid membrane was suppressed in both the *stn7* mutant and membranes that were unable to form a pH gradient (Fig. 3 *D*). Furthermore, we observed that the thylakoid did not return to the original state upon turning off the PSII-specific light. This is likely the result of the absence of stromal proteins and/or molecules that were removed during thylakoid isolation.

Our results indicate that at least two mechanisms control the height change. It has been reported that upon illumination of *Arabidopsis* leaves with white light, there is a 17% increase in the stacking repeat distance of thylakoids due to lumen expansion, and that uncoupling the pH gradient suppresses this effect (10). This value (17%) is comparable to the height increase found in this investigation using isolated thylakoids (22 ± 12% (mean ± SD), Fig. 1 *C*), and we also observed that the height change depended on the pH gradient, suggesting that lumen expansion may account for this change. Because there is a significant delay in the height change, the pH gradient, which forms within seconds of illumination (26,27), cannot be sufficient to cause this effect.

Our observation that the height change was suppressed in the *stn7* mutant (Fig. 3 *D*) indicates that STN7-dependent phosphorylation also contributes to the height change phenomenon when samples are illuminated with PSII-specific light. This is possibly caused by the partial unstacking of thylakoid membranes, which is thought to occur through disruption of stroma-face interactions between LHCII trimers upon phosphorylation (25,28) leading to lumen expansion by disruption of grana membrane bridges as suggested by Chuartzman et al. (6). Another possibility is that the phosphorylation of LHCII may cause lumen expansion by altering supercomplex organization and thereby affecting interactions between lumen-exposed proteins (7,29).

The magnitude of height change in the various samples leads us to believe that the pH-dependent and STN7-dependent components of this change function in concert. We propose that lumen expansion or swelling of the thylakoid membrane is the driving force behind the height increase, and when the molecular interactions that normally hold the grana stacks together are removed by phosphorylation, this swelling can manifest as an even greater height change (Fig. 4). The larger variability seen for the WT samples after light treatment, in both the EM-based measurements of the packing repeat of the membrane stacks and the AFM-based height measurements, is indeed suggestive of unstacking or release of constraints associated with LHCII phosphorylation.

In contrast to the changes in height, the increase in elasticity does not require STN7-dependent LHCII phosphorylation or unstacking (Fig. 3 *C*). In fact, we observed that the elasticity increase appeared to be greater in the *stn7* mutant compared to the WT. Formation of the pH gradient was responsible for a large fraction of the elasticity change, as shown by the effect of gramicidin D (Fig. 3 *C*). The stiffening also differed from the height change in that it did not have a time delay but rather occurred immediately upon illumination (Fig. 2 *A*). The immediate response in elasticity is consistent with it being driven by the formation of the pH gradient. We argue that the unstacking seen in WT membranes, which allows the height change, also attenuates the stiffening effect by releasing constraint on the membrane and can explain the larger elasticity increase seen in *stn7*. Because a two- to threefold increase in elasticity remained even in the presence of gramicidin D, it is possible that other light-dependent changes contribute to the observed stiffening, and the mechanism of this stiffening remains to be determined.

State transitions have been proposed to balance excitation between the two photosystems by decreasing the cross section of PSII and increasing the cross section of PSI (4). When LHCII is primarily associated with PSII, a plant is said to be in state 1. When PSII is preferentially excited relative to PSI, a portion of the LHCII complexes migrate through the membrane and can attach to PSI (state 2). Phosphorylation of LHCII by STN7 is thought to cause this rearrangement by promoting the unstacking of the grana membranes, which facilitates the movement of LHCII

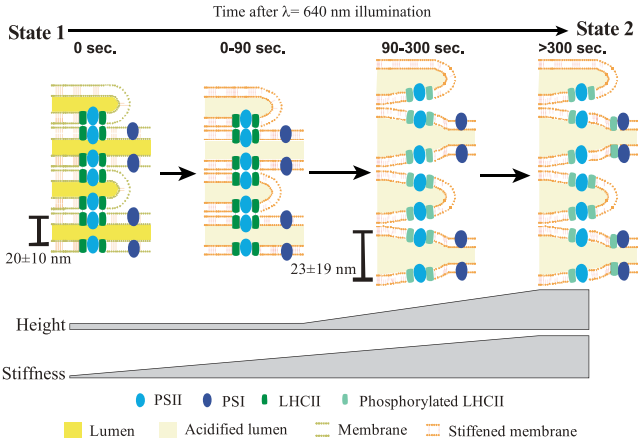

FIGURE 4 Proposed model of thylakoid membrane response to PSII-specific illumination. Before illumination, thylakoids are in state 1, and then an intermediate state (0–90 s) occurs as the membrane begins to stiffen (*depicted by a change in membrane color*) in response to formation of the pH gradient. Next, lumen expansion and swelling occur (90–300 s), driven by LHCII phosphorylation and membrane unstacking, while further membrane stiffening takes place. Finally, migration and association of phosphorylated LHCII with PSI result in establishment of state 2. To see this figure in color, go online.

complexes (17). Although the change from state 1 to state 2 occurs within 10 to 20 min in plants, it has recently been shown that STN7 is also important under fluctuating light and this function is independent of LHCII migration (30). Our results suggest that the unstacking of membranes is an intermediate state in the process of thylakoid regulation, occurring within a few minutes (Fig. 4). Lumen expansion has been proposed to facilitate plastocyanin diffusion between the cytochrome b_6f complex and PSI, which could improve electron transport (10,12). Our observation that the height increase is larger in WT than in *stn7* thylakoids (Fig. 3, *A* and *B*), suggests that unstacking of the membrane caused by PSII-specific illumination may facilitate not only LHCII migration, but also further enhance plastocyanin diffusion and help relieve excitation pressure on PSII.

This work also addresses the question of what causes lumen expansion upon exposure to PSII-specific illumination. If decoupling of membrane proteins from one another allowed influx of water, one would expect that the elasticity would decrease, however we did not observe this trend during our experiments (Figs. 2 and 3). Therefore, we argue that it is most likely an intermembrane interaction within the lumen that causes the lumen expansion and the stiffening of the thylakoid membrane we observe. Whether this is an attractive force between membranes that is disrupted during illumination or a repulsive force that is shielded in the dark remains to be determined.

Both the attractive and repulsive forces between grana membranes have been explored previously and protein components were implicated in these interactions (31). The oxygen-evolving complex (OEC) within the lumen is an intriguing candidate for facilitating this interaction. The OEC is the largest lumenal protrusion and is thought to be the main determinant of lumenal spacing (32). It has been proposed that the PsbQ protein of the OEC is involved in facilitating protein-protein interactions between OECs on opposing membranes (33). However, the positioning of OECs on opposing lumenal surfaces with respect to each other is an open question due largely to the varying estimates of lumen spacing (34). Some reports have indicated that the lumen spacing presents no spatial hindrance to OECs being directly opposite one another (32). In contrast, others have suggested that this arrangement would not be possible in the dark, where an offset arrangement would be more likely, and that a lumen expansion would be needed to facilitate plastocyanin diffusion (10,12). The stiffening of the membrane fits this view, as a stiff membrane, together with a lumen expansion, would be expected to interfere less with plastocyanin diffusion.

CONCLUSIONS

In conclusion, we have characterized for the first time, to our knowledge, the dynamic changes in height, elasticity, and viscosity of isolated thylakoid membranes in response to different illumination, drugs, and mutations using AFM. We found that upon illumination of WT thylakoids, the elasticity of the membrane increased immediately, followed by a height increase with a light intensity-dependent delay. The height as well as the elasticity increase could be reduced by the addition of the uncoupler gramicidin D. These results indicate that a major molecular mechanism controlling the elasticity and height change of thylakoids is the pH gradient across the membrane, which drives lumen expansion by altering the grana membrane interactions. Using the *stn7* mutant we further showed that in the absence of grana unstacking the height increase is suppressed but the elasticity increase was larger. These results indicate that STN7-dependent phosphorylation releases constraints on the membrane and allows the lumen to expand further. Based on these results we propose a mechanistic explanation to support the role of state transitions in rapid acclimation to light changes.

SUPPORTING MATERIAL

Six figures and derivation of Eq. 1 are available at http://www.biophysj.org/biophysj/supplemental/S0006-3495(14)00929-6.

This research was supported by the Division of Chemical Sciences, Geosciences, and Biosciences, Office of Basic Energy Sciences, Office of Science, U.S. Department of Energy, FWP No. SISGRKN. K.K.N. was funded by the Howard Hughes Medical Institute and the Gordon and Betty Moore Foundation (through grant GBMF3070). C.H.C. was funded by the Villum Kann Rasmussen foundation (grant 495289).

REFERENCES

1. Niyogi, K. K. 1999. PHOTOPROTECTION REVISITED: genetic and molecular approaches. *Annu. Rev. Plant Physiol. Plant Mol. Biol.* 50:333–359.
2. Horton, P., and A. Ruban. 2005. Molecular design of the photosystem II light-harvesting antenna: photosynthesis and photoprotection. *J. Exp. Bot.* 56:365–373.
3. Standfuss, J., A. C. Terwisscha van Scheltinga, …, W. Kühlbrandt. 2005. Mechanisms of photoprotection and nonphotochemical quenching in pea light-harvesting complex at 2.5 A resolution. *EMBO J.* 24:919–928.
4. Minagawa, J. 2011. State transitions—the molecular remodeling of photosynthetic supercomplexes that controls energy flow in the chloroplast. *Biochim. Biophys. Acta.* 1807:897–905.
5. Allen, J. F., and J. Forsberg. 2001. Molecular recognition in thylakoid structure and function. *Trends Plant Sci.* 6:317–326.
6. Chuartzman, S. G., R. Nevo, …, Z. Reich. 2008. Thylakoid membrane remodeling during state transitions in Arabidopsis. *Plant Cell.* 20:1029–1039.
7. Dietzel, L., K. Bräutigam, …, T. Pfannschmidt. 2011. Photosystem II supercomplex remodeling serves as an entry mechanism for state transitions in Arabidopsis. *Plant Cell.* 23:2964–2977.
8. Johnson, M. P., T. K. Goral, …, A. V. Ruban. 2011. Photoprotective energy dissipation involves the reorganization of photosystem II light-harvesting complexes in the grana membranes of spinach chloroplasts. *Plant Cell.* 23:1468–1479.
9. Albertsson, P.-Å. 2001. A quantitative model of the domain structure of the photosynthetic membrane. *Trends Plant Sci.* 6:349–358.

10. Kirchhoff, H., C. Hall, …, Z. Reich. 2011. Dynamic control of protein diffusion within the granal thylakoid lumen. *Proc. Natl. Acad. Sci. USA.* 108:20248–20253.

11. Rozak, P. R., R. M. Seiser, …, R. R. Wise. 2002. Rapid, reversible alterations in spinach thylakoid appression upon changes in light intensity. *Plant Cell Environ.* 25:421–429.

12. Kirchhoff, H., S. Lenhert, …, J. Nield. 2008. Probing the organization of photosystem II in photosynthetic membranes by atomic force microscopy. *Biochemistry.* 47:431–440.

13. Sznee, K., J. P. Dekker, …, R. N. Frese. 2011. Jumping mode atomic force microscopy on grana membranes from spinach. *J. Biol. Chem.* 286:39164–39171.

14. Yamada, T., H. Arakawa, …, A. Ikai. 2002. Use of AFM for imaging and measurement of the mechanical properties of light-convertible organelles in plants. *Ultramicroscopy.* 91:261–268.

15. Kaftan, D., V. Brumfeld, …, Z. Reich. 2002. From chloroplasts to photosystems: in situ scanning force microscopy on intact thylakoid membranes. *EMBO J.* 21:6146–6153.

16. Scheuring, S., and J. N. Sturgis. 2005. Chromatic adaptation of photosynthetic membranes. *Science.* 309:484–487.

17. Bellafiore, S., F. Barneche, …, J. D. Rochaix. 2005. State transitions and light adaptation require chloroplast thylakoid protein kinase STN7. *Nature.* 433:892–895.

18. Casazza, A. P., D. Tarantino, and C. Soave. 2001. Preparation and functional characterization of thylakoids from *Arabidopsis thaliana*. *Photosynth. Res.* 68:175–180.

19. Stark, R. W., T. Drobek, and W. M. Heckl. 2001. Thermomechanical noise of a free v-shaped cantilever for atomic-force microscopy. *Ultramicroscopy.* 86:207–215.

20. Emerson, R., and M. L. Charlton. 1943. The dependence of the quantum yield of chlorella photosynthesis on wave length of light. *Am. J. Bot.* 30:165–178.

21. Mahaffy, R. E., S. Park, …, C. K. Shih. 2004. Quantitative analysis of the viscoelastic properties of thin regions of fibroblasts using atomic force microscopy. *Biophys. J.* 86:1777–1793.

22. McDonald, K. L., and R. I. Webb. 2011. Freeze substitution in 3 hours or less. *J. Microsc.* 243:227–233.

23. Ludtke, S. J., P. R. Baldwin, and W. Chiu. 1999. EMAN: semiautomated software for high-resolution single-particle reconstructions. *J. Struct. Biol.* 128:82–97.

24. Frank, J., M. Radermacher, …, A. Leith. 1996. SPIDER and WEB: processing and visualization of images in 3D electron microscopy and related fields. *J. Struct. Biol.* 116:190–199.

25. McDonnel, A., and L. A. Staehelin. 1980. Adhesion between liposomes mediated by the chlorophyll *a/b* light-harvesting complex isolated from chloroplast membranes. *J. Cell Biol.* 84:40–56.

26. Po, E. S. M., and J. W. Ho. 1997. Paraquat affects light-induced proton transport through chloroplast membranes in spinach. *Comp. Biochem. Phys. C.* 118:65–69.

27. Rumberg, B., and H. Muhle. 1976. Investigation of kinetics of proton translocation across thylakoid membrane. *Bioelectrochem. Bioenerg.* 3:393–403.

28. Barber, J. 1982. Influence of surface charges on thylakoid structure and function. *Annu. Rev. Plant Physiol.* 33:261–295.

29. Daum, B., D. Nicastro, …, W. Kühlbrandt. 2010. Arrangement of photosystem II and ATP synthase in chloroplast membranes of spinach and pea. *Plant Cell.* 22:1299–1312.

30. Tikkanen, M., M. Grieco, …, E. M. Aro. 2010. Thylakoid protein phosphorylation in higher plant chloroplasts optimizes electron transfer under fluctuating light. *Plant Physiol.* 152:723–735.

31. Albertsson, P.-Å. 1982. Interaction between the lumenal sides of the thylakoid membrane. *FEBS Lett.* 149:186–190.

32. Kouřil, R., G. T. Oostergetel, and E. J. Boekema. 2011. Fine structure of granal thylakoid membrane organization using cryo electron tomography. *Biochim. Biophys. Acta.* 1807:368–374.

33. De Las Rivas, J., P. Heredia, and A. Roman. 2007. Oxygen-evolving extrinsic proteins (PsbO,P,Q,R): bioinformatic and functional analysis. *Biochim. Biophys. Acta.* 1767:575–582.

34. Dekker, J. P., and E. J. Boekema. 2005. Supramolecular organization of thylakoid membrane proteins in green plants. *Biochim. Biophys. Acta.* 1706:12–39.

SUPPLEMENTARY MATERIALS

For

Dynamic mechanical responses of *Arabidopsis* thylakoid membranes during PSII-specific illumination

by C. H. Clausen et al.

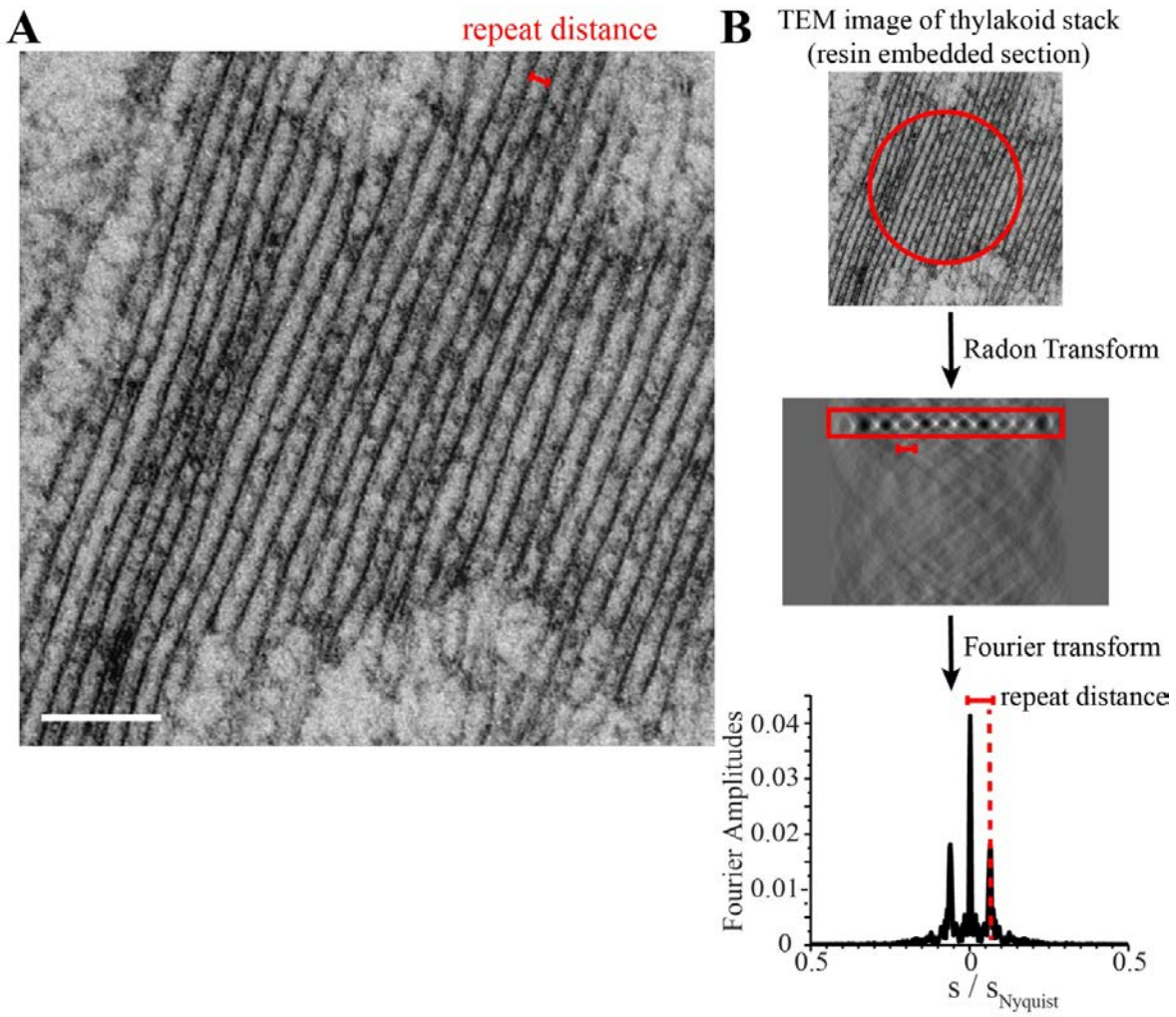

Figure S1: Stacking repeat distance measurements from EM images (resin embedded sections) (A) Detail of a TEM image of high-pressure frozen freeze-substituted section through a thylakoid stack showing the characteristic repeat motif. The repeat marked in red includes two membrane bilayers, the stromal and the lumenal spaces. As illustrated here, the stromal space or "partition gap" cannot be distinguished from the membrane bilayers (dark stripe). (B) Repeat distance measurement: the characteristic stacking repeat was measured for each thylakoid (top) by finding the peaks in the Fourier transform of its Radon transform. Scale bar is 100nm.

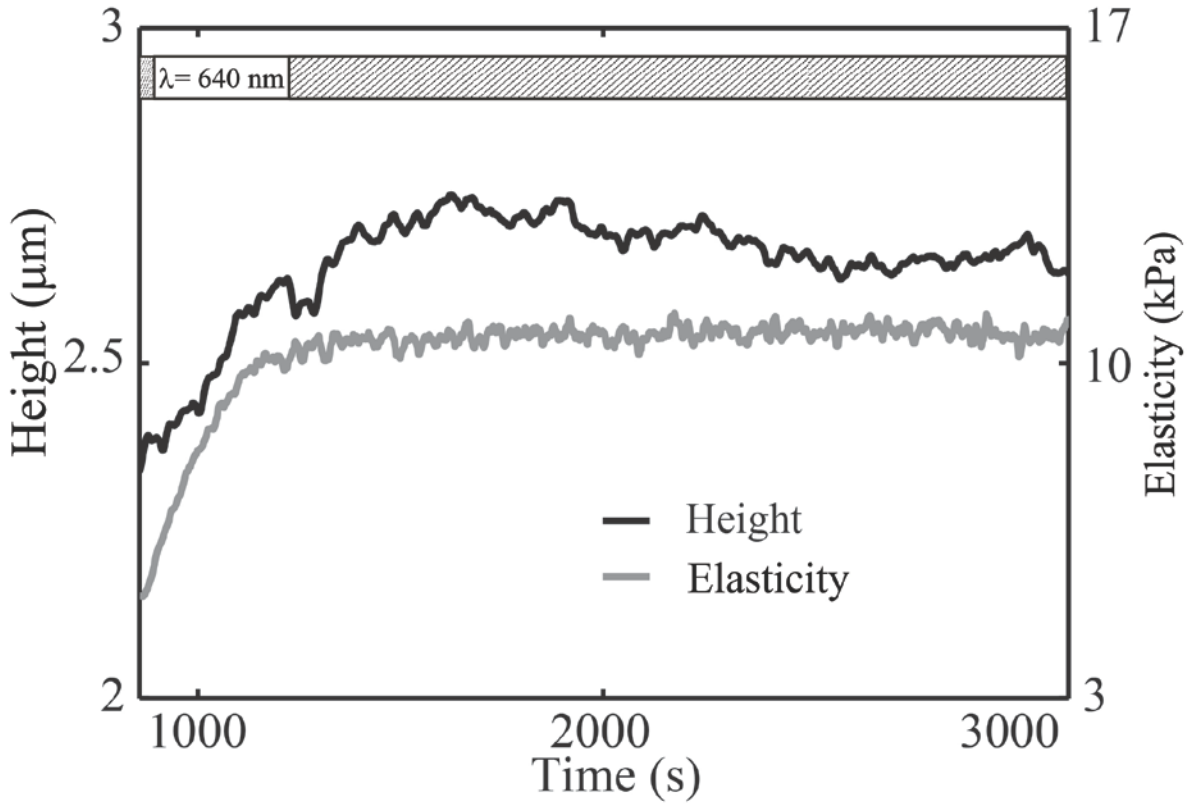

Figure S2: Plot of the normalized stiffness and height of a wild-type thylakoid membrane illuminated for 6 min followed by 30 min in the dark. Neither the stiffness nor the height show a significant change after λ=640 nm illumination is turned off within this time span.

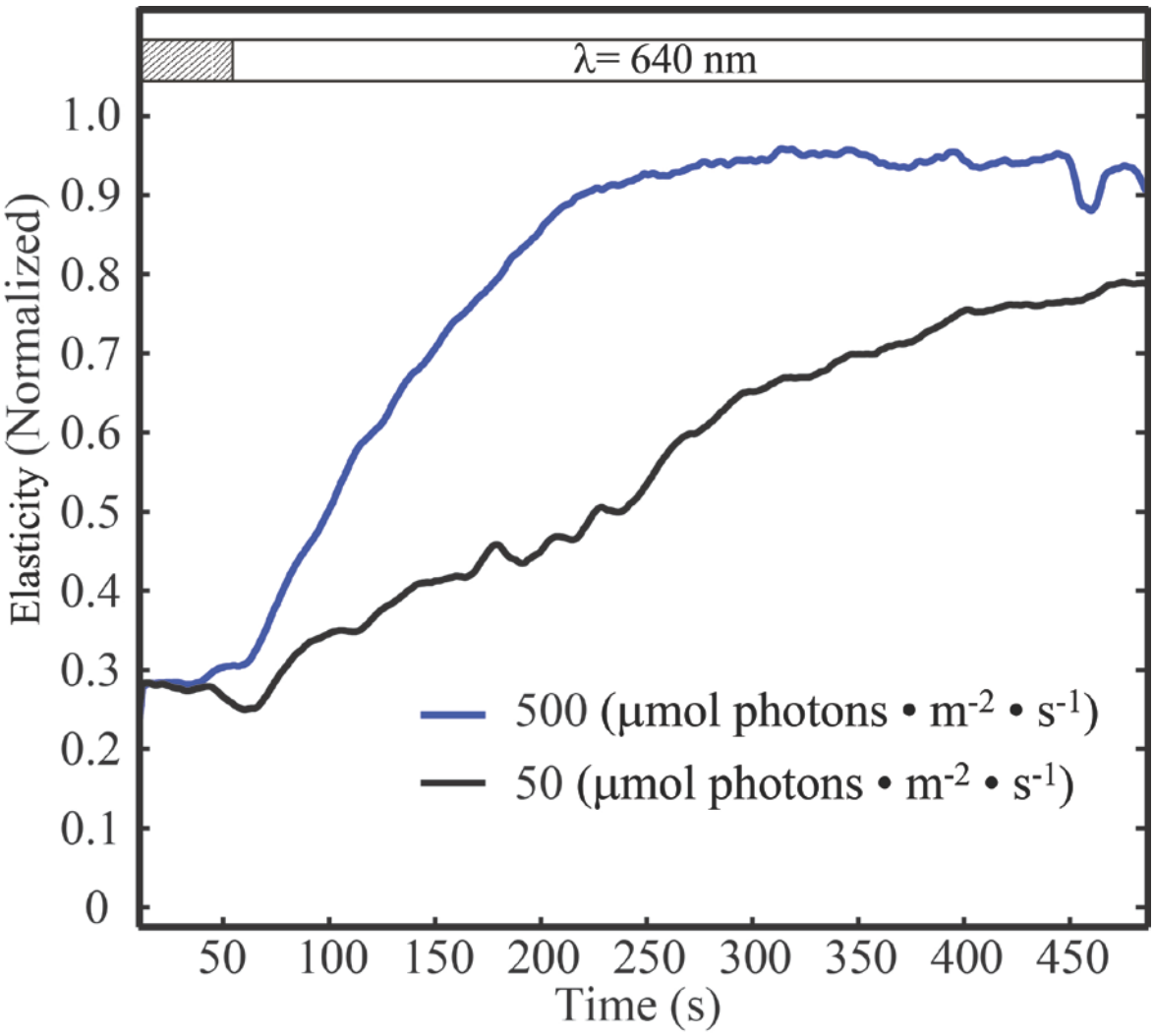

Figure S3: Plot of the normalized stiffness from wild-type thylakoid membranes illuminated with 640 nm light at different intensities. The plot shows that the stiffness response time (t_r) is greater at higher light intensity.

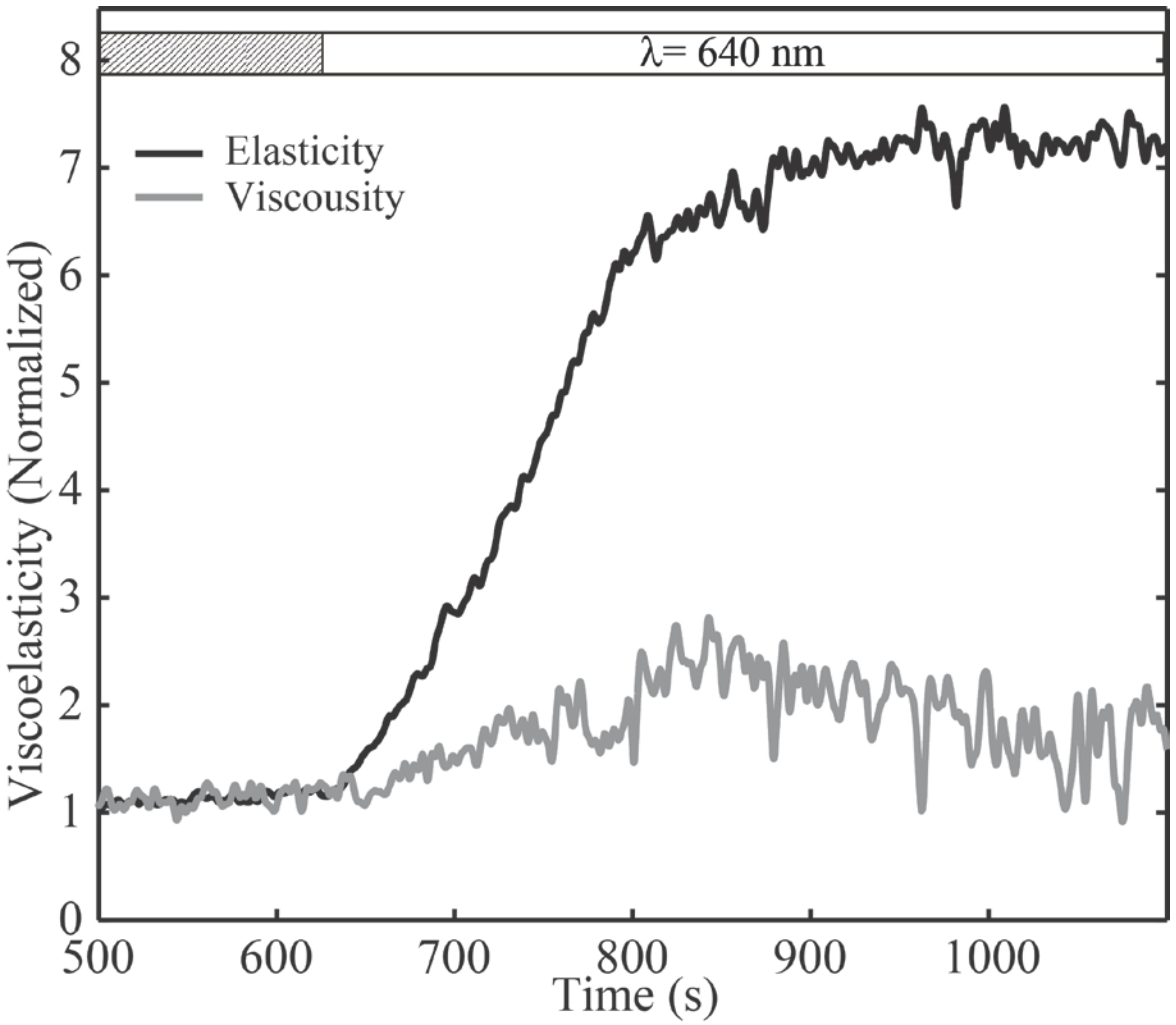

Figure S4: The viscoelasticity of a single measurement calculated according to Eq. 1. The elastic and viscous moduli are normalized to their initial values. Changes in G" in response to λ=640 nm illumination are less significant than in G'.

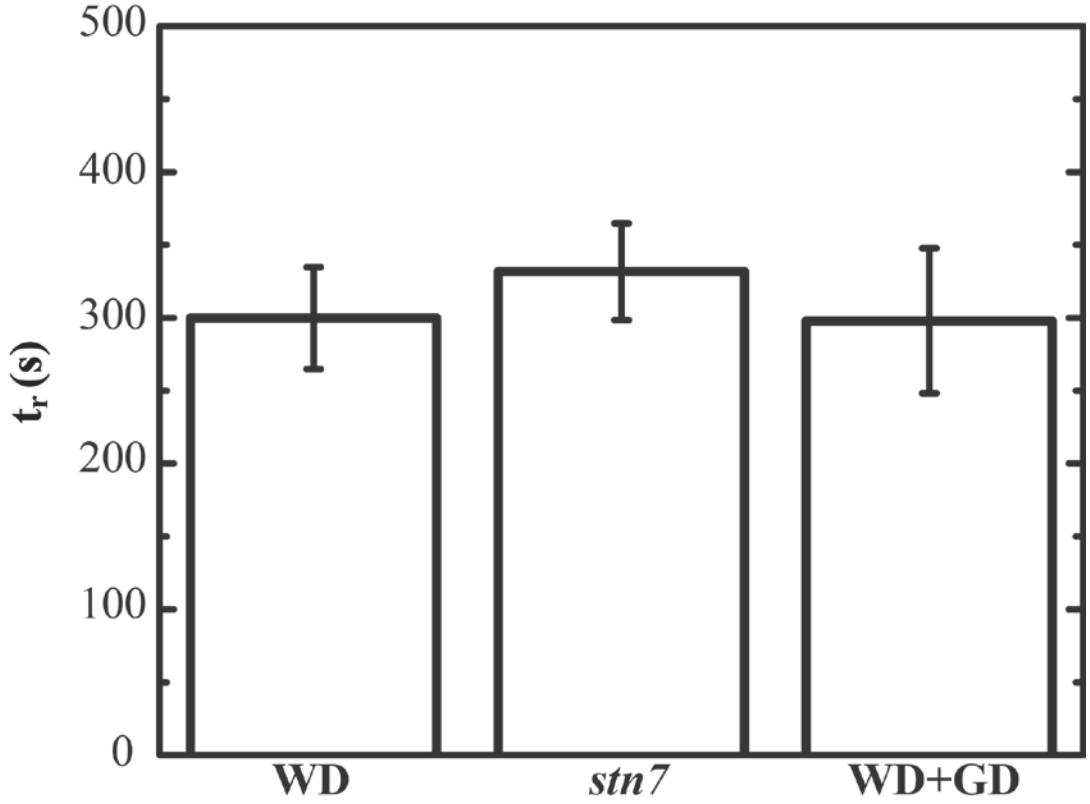

Figure S5: Histogram plot of the stiffness response time (t_r) in seconds for wild type (WT), *stn7*, and wild type treated with gramicidin D (WT + GD). The response time does not depend on the presence of STN7 or formation of the pH gradient.

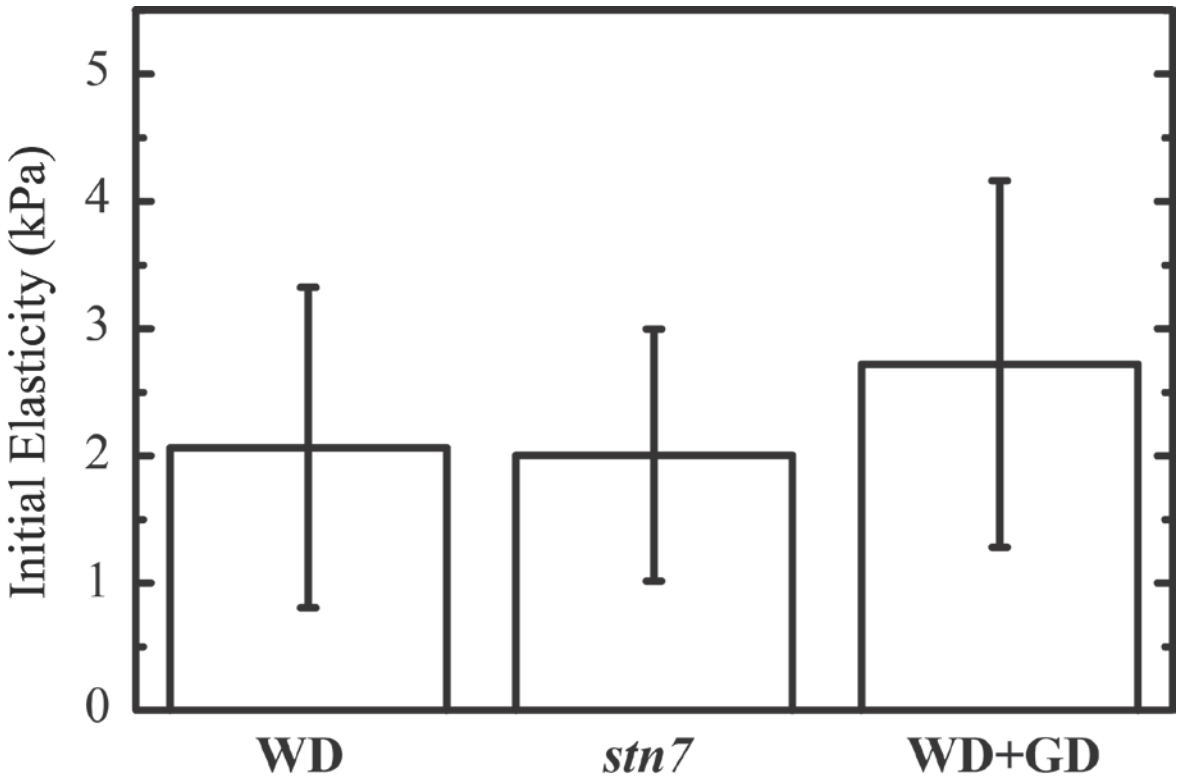

Figure S6: The initial elasticity (G') of wild type (WT), *stn*7 mutant, and gramicidin D (GD) treated thylakoid membranes before PSII illumination. There is no significant difference between all different samples.

Derivation of Equation 1:

Using Equation 5 from Mahaffy *et al.* 2004

$$K_1^* = \frac{f_{osc}^*}{2\delta^*(R\delta_0)^{\frac{1}{2}}}$$

combined with the definitions $K = \frac{E}{1-\nu^2}$ and $G = \frac{E}{2(1+\nu)}$, we obtain

$$G^* = \frac{(1-\nu)f_{osc}^*}{4\delta^*(R\delta_0)^{\frac{1}{2}}} ,$$

where f_{osc}^* and δ^* are complex numbers describing force and displacement, respectively, that depend on angular frequency ω and phase ϕ. For negligible drag, which we confirmed for the frequencies used in our experiments, the applied force is given by

$$f_{osc}^* = k \cdot A \cdot \exp\big(i(\omega t + \phi)\big) ,$$

where k is the spring constant of the cantilever and A is the measured cantilever amplitude. The indentation is given by

$$\delta^* = \delta \cdot \exp(i\omega t) ,$$

where δ is the applied amplitude minus the measured amplitude. Combining the equations for G^*, $f_{osc}{}^*$, and δ^*, we obtain

$$G^* = \frac{(1-\nu)*k*A*\exp\big(i(wt+\phi)\big)}{4*\delta*\exp(iwt)*(R\delta_0)^{\frac{1}{2}}} = \frac{(1-\nu)\cdot k\cdot A}{4\cdot\delta\cdot\sqrt{R\delta_0}} \cdot \exp(i\cdot\phi) ,$$

which is the form used in Equation 1 in the text.